PARTIAL DISCHARGES

DETECTING PARTIAL DISCHARGES

Why Discharge Detection?

Detection of partial discharges is particularly suited for locating one small defect in an otherwise perfect dielectric, where one single defect may be as dangerous as a multitude of defects. This is of particular interest in dielectrics where single defects readily occur. Examples are extruded dielectrics, like polyethylene, or cast materials, like epoxy resin. With actual detection techniques, a defect as small as 10 by 100 μm is detected, so that partial discharge detection has grown into an indispensable tool for evaluating high-voltage insulation.

In lapped paper insulation, either no defect or hundreds of thousands of cavities occur at a time, and a combined action of discharges is expected. These discharges are usually measured with dielectric loss measurement techniques, like the Schering bridge; see DIELECTRIC MEASUREMENT. However, conventional discharge detection is also applied to paper insulated equipment, such as ac power transformers or high-voltage dc submarine cables.

Bases for Detection

Detection of partial discharges is based on observing their physical effects (1). These effects are *electrical* or *nonelectrical.* The detection of electrical effects covers the majority of all partial discharge tests. In particular, charge displacement in the dielectric circuit is used for detection. The customary unit for describing the magnitude of discharges, the *picocoulomb,* is derived from this charge displacement; see the later section on evaluating ac discharges.

Detecting nonelectrical effects, however, should not be ignored. It forms a valuable extension to the usual electrical discharge detection. Two of the nonelectrical methods are of practical importance: acoustical detection and optical detection. These two are discussed in the following section.

NONELECTRICAL DETECTION

Acoustical Detection, General

Acoustical or noise detection is most effective when locating partial discharges in air, such as coronas at sharp points or surface discharges at the exterior of insulators. Discharges in solid or oil-impregnated dielectrics are also detected, but they suffer from the heavy attenuation of acoustic waves in dielectric materials. An important drawback of acoustical detection is that readings cannot be expressed in picocoulombs as is customary in electrical tests.

Audible Noise in Air

The detection of discharges by ear is simple but insensitive. Discharges of some hundred picocoulombs are detected by ear, but the least ambient noise increases this level to several hundreds of picocoulombs. The method should not, however, be underestimated. If surface discharges of sufficient amplitude are present, observation by ear adequately locates their position. Simple aids like a trumpet-shaped tube are used to improve sensitivity and locating power.

Ultrasonic Detection in Air

Better results are obtained by detecting the *ultrasonic* noise of the discharges. The ultrasonic spectrum is preferred, because the environmental noise in the ultrasonic spectrum is far lower than in the audible range. A narrow band of 30 kHz to 50 kHz is a good option. At higher frequencies, attenuation of sound waves in air is too large. Ultrasonic devices in this

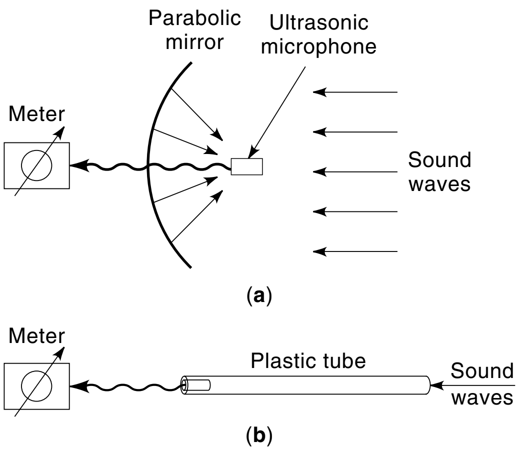

Figure 1. Acoustical discharge detection in air (9): (a) With a parabolic mirror, the sound waves are focused on an ultrasonic microphone. (b) With a plastic tube, a more accurate location is achieved.

category are commercially available (2). A parabolic mirror concentrates sound waves in an ultrasonic microphone. The signals are converted to audible sound and are read from a decibel meter (see Fig. 1). Note, however, that the decibel meter does not present the discharges in picocoulombs. The discharge is located within an angle of about 10°. Discharges are more accurately located with a plastic tube, one to two meters long and a few centimeters in inside diameter. An ultrasonic microphone at the end of the tube serves as a detector (see Fig. 1).

The acoustical methods presented here are excellent aids for trouble-shooting. They uncover unwanted discharges, such as corona or surface discharges, and corrective measures are readily taken.

Ultrasonic Detection in Oil-Impregnated Equipment

Internal discharges are sometimes detected by placing sensors at the tank of oil-impregnated components, such as power transformers or switchgear (see Fig. 2). An alternative is to immerse hydrophones in the insulating oil (see Fig. 2). The noise signals are amplified and displayed at a 50 (60) Hz time base (3). This has the advantage that the signals from electrical discharges are synchronized, whereas disturbing signals from other sources are moving over the time base. This also helps to *recognize* discharges by electrical detection

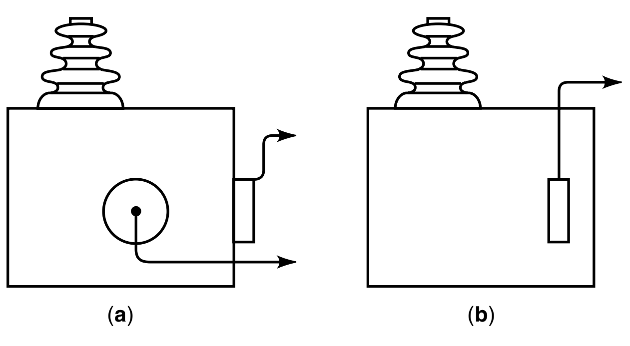

Figure 2. Acoustical discharge detection in oil. Sensors are placed on the tank or immersed in the oil (9).

(28) as discussed later. Disturbances exist, however, which synchronize with the power frequency, such as magnetostrictive noise from the transformer core. These disturbances are suppressed by observing the acoustic signals at a fairly high frequency, say 100 kHz, with a bandwidth of some tens of kilohertz. Discharges in oil-impregnated transformers are also *located* by acoustical detection (24).

Ultrasonic Detection in Solids

Discharge detection in solid insulation is sometimes performed by placing ultrasonic transducers at the sample surface. The sensitivity is usually unsatisfactory because of the high attenuation of sound waves in solids. Nevertheless, tests have been made with power capacitors, power cables, and machine coils with a reported sensitivity of some hundreds of picocoulombs (1).

Ultrasonic Detection in Compressed-Gas Insulation

Ultrasonic detection in gas-insulated switchgear (GIS) is more successful. Corona at unwanted protrusions and surface discharges along the spacers are detected with a sensitivity of about 25 pC. Moreover, unwanted particles that do not discharge, but move in the dielectric gas, are also detected (4). Discharges and particles are located within a distance of about 30 cm.

Optical Detection, General

The use of light detection is even more limited. Only corona and surface discharges are observed. In these restricted cases, however, light detection is most powerful. It locates discharges within millimeters and it offers sensitivities which surpass those of electrical detection. It requires, however, a test place shielded from ambient light. Moreover, it has the same disadvantage as noise detection. The results are not expressed in picocoulombs.

Visual Detection

The human eye is quite sensitive to light, especially after adapting to darkness for about 15 min. Discharges of a few hundred picocoulombs are detected and located without any optical aids (1).

Photographic Detection

A sample is placed in a darkroom and the shutter of a camera is opened for a time, during which high voltage is applied to the sample. In addition, the sample is illuminated for a short time so that a picture is obtained in which the discharges are superimposed on the sample profile (see Fig. 3). The sensitivity of the method varies with exposure time. Surface discharges from 1 pC upward are detected with an exposure time of several hours. A corona is more concentrated. A corona of about 20 pC is, therefore, recorded in a few minutes. Locating discharges by this method is excellent.

The restriction to discharges at a sample surface is sometimes evaded by using translucent materials like plastic or glass. Figure 4 shows an example used for locating discharges along cable terminations.

Photographic detection is an excellent aid in trouble-shooting. It locates unwanted discharges, so that corrective measures can be taken.

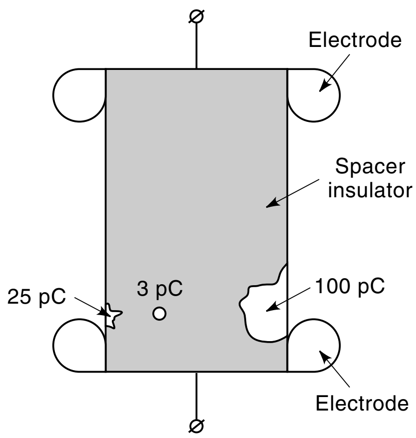

Figure 3. Photographic detection of surface discharges on a spacer insulator (1). The area covered by the discharge is some measure for the discharge magnitude.

Light Amplification

Extremely high sensitivities are obtained with photomultipliers. Electrical discharges radiate mainly in the ultraviolet spectrum, and photomultipliers are available with a high gain in the ultraviolet spectrum. Sensitivites of 0.05 pC and possibly 0.005 pC are reported (5). The results are well presented on a 50 (60) Hz timescale, which helps to recognize discharges and to distinguish between wanted and unwanted signals. However, location is not achieved with photomultipliers.

Good results are also obtained with *image intensifiers* coupled to a photo or video camera (6). In this case, both high *sensitivity* and good *location* are achieved, also with the restrictions previously stated.

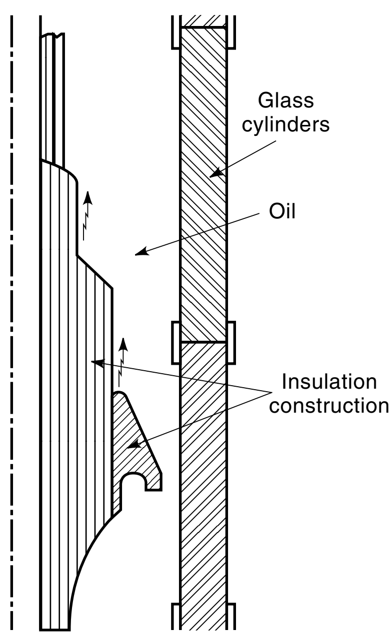

Figure 4. Photographic detection of discharges in a cable terminal through glass cylinders (1).

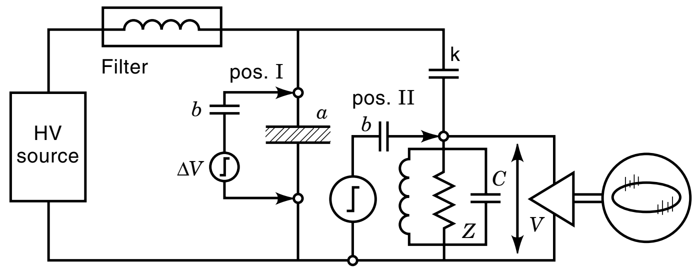

Figure 5. Straight detection circuit for both ac and dc discharges. Sample a is grounded. Calibration must be performed at the terminals of sample a (9). The detected pulse V is amplified and observed in the observation unit O.

ELECTRICAL DETECTION

Conventional Detection at Ac and Dc Voltage

Any circuit for detecting electrical discharges can be reduced to the basic circuit shown in Fig. 5. A circuit in which one of the elements is missing does not operate properly. In the circuit of Fig. 5, charges are displaced, which cause voltage impulses over the measuring impedance Z. These impulses are amplified and presented to an observation unit O, which may consist of an oscilloscope and/or a digital analyzer. The coupling capacitor k is essential and is of the same order of magnitude as the sample. Too small a value of k causes loss of sensitivity (1).

Balanced Detection

The circuit of Fig. 5 is a straight detection circuit. The alternative is the balanced circuit of Fig. 6, which has the advantage of rejecting unwanted pulses from the high-voltage source or other external noise. Two samples are measured at a time. The variable elements in the lower bridge arms are

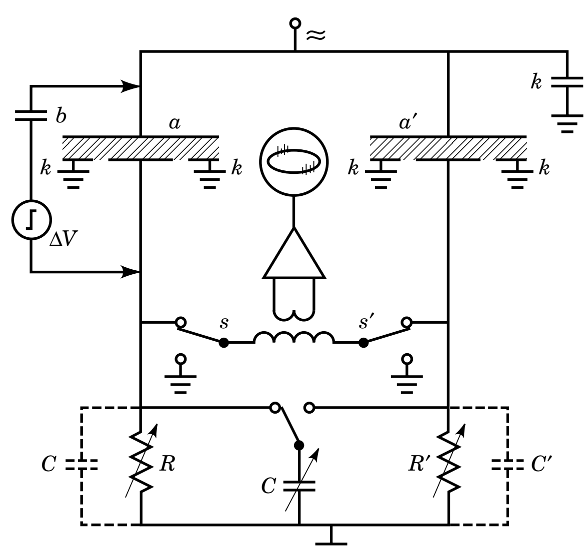

Figure 6. Balanced detection for both ac and dc discharges (9). Discharges in the samples a and a' are detected. Discharge signals from outside (from the capacitance k or the HV source) are rejected. The bridge is balanced by adjusting R, R', and C. Calibration is performed by injecting a standard charge into the sample.

adjusted so that the response to external noise is minimal. External interference may be reduced by as much as 5000 times.

Both types of conventional detectors, straight and balanced, are covered by the international IEC 270 standard (18).

Calibration

Calibration in both cases is performed by injecting charges of known magnitude into the sample. Electronic charge generators are commercially available for that purpose. The calibrating discharge is always injected into the sample, notwithstanding the more complicated procedure. Built-in calibrators at the low voltage side of the detector cause appreciable errors. The calibration procedure is amply described in IEC 270 (17). Revisions are prepared in (18), especially with a view to digital processing of measuring results.

Bandwidth and Display

The bandwidth of the conventional detectors previously discussed is usually of the order of 100 to 400 kHz. Ac discharges are displayed on a 50 (60) Hz time base, where they are satisfactorily analyzed (see Fig. 7). Dc discharges are displayed in another way, preferably as in Fig. 20.

Time-Resolved Detection

An alternative method, frequently used for research purposes, is the ultrawide band or time-resolved detection (6,11). Ac or dc discharge impulses are amplified with a bandwidth of 100 MHz to more than 500 MHz. Their shape is related to the physical nature of the discharges as discussed later.

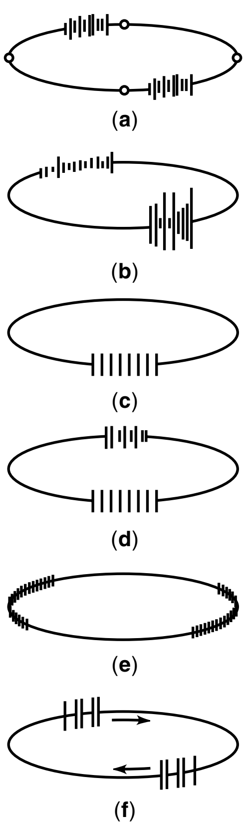

Figure 7. ac discharge patterns (a) to (f) which are characteristic for certain discharge origins (9).

OBSERVATION OF AC DISCHARGES

Discharge Patterns

Ac discharge impulses are displayed on a 50 (60) Hz time base. This time base is usually arranged as an ellipse, where the ends O correspond to the zero points of the high ac voltage (see Fig. 7). The top (+) and bottom (−) of the ellipse correspond to the crests of the ac high voltage. Because partial discharges are well synchronized to the ac test voltage, they appear at the ellipse as reasonably stable impulses. The highest of the discharge impulses is measured and is usually called the *discharge magnitude.*

The discharge patterns seen on the ellipse are usually characteristic of the type of discharge under observation. Different discharge types are recognized this way (7), as shown in Fig. 7. Pattern (a) is characteristic of a cavity completely surrounded by a dielectric. Then the discharges at both sides are equal or do not differ by more than a factor of 3 (these patterns also make it possible to distinguish between discharges bounded by an earth electrode and those bounded by a high voltage electrode). Pattern (b) in Fig. 7 is characteristic of discharges bounded at one side by an electrode. The discharge impulses at both sides differ by more than a factor of 3. Pattern (c) shows negative *corona.* All impulses are of the same magnitude and they occur only at one polarity. At higher voltages, some positive corona appears at the other side of the ellipse. Pattern (d) shows a corona in oil, a characteristic pattern at one side and indistinct discharges at the other. Pattern (e) shows contact noise in the leads, an indistinct noise pattern at the zero points where the capacitive current is maximal. Pattern (f) shows floating parts, metallic parts in the dielectric that make bad contacts with the electrodes. This causes regularly repeating discharge groups which rotate along the ellipse.

Phase-Related Information

All information in these diagrams is expressed by the phase angle φ and the discharge magnitude q at any moment (see Fig. 16). This relates to discharges of ac voltage (in contrast to discharges of dc). This fact is used, in a later section, for computer-aided recognition of discharges.

Voltage Diagrams

When observing discharges, making a diagram of the discharge magnitude in picocoulombs as a function of the test voltage in kilovolts, as shown in Fig. 8(a), is strongly recommended. Many discharge detectors and analyzers plot these diagrams automatically (2,26,27). The shape of these diagrams is also characteristic of the type of discharge and helps in recognizing the discharges under test (9). Surface discharges usually show an increasing discharge magnitude, because there is ample space for the discharges to grow when the voltage is increased. The same applies to large cavities and fissures in the dielectric. Small cavities are completely filled by discharges after a certain voltage is reached, and the discharge magnitude remains the same. Coronas give distinc-

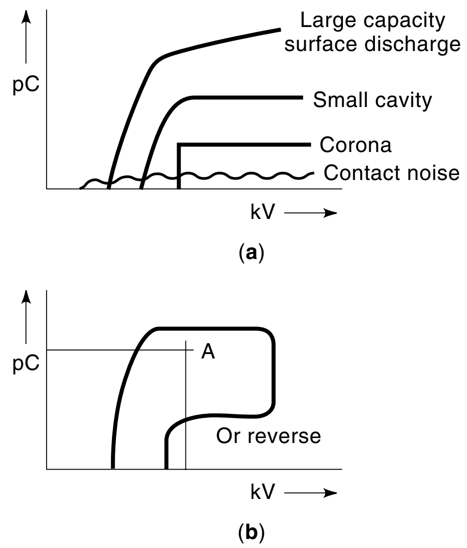

Figure 8. (a) Discharge diagrams may add to the recognition of ac discharges. (b) A discharge limit **A** may be set, where the discharges are not allowed to be larger than specified (9).

tive square diagrams. The diagram also differs for increasing and decreasing voltage, as shown in Fig. 8(b).

The combination of discharge patterns, as in Fig. 7, and voltage diagrams, as in Fig. 8 in many cases answer the question of which type of discharge is under observation. This analysis, however, covers a limited number of discharge types and it requires an experienced operator. Much progress has been made by digital analysis of the $q = f(\varphi)$ information, as discussed later.

Detection and Observation of Dc Discharges

Stages in Dc. First of all it is ascertained whether the field in the sample is actually a dc field (10). In the diagram of Fig. 9, stage III is the only one with a pure dc field. Stage I is pure ac with ac driven discharges. Stages II and IV are transitional, where a mixture of ac and dc discharges are found.

Detection of Dc Discharges. Dc voltage discharges are detected in the same way and with the same detectors as ac (10). Conventional discharge detectors (see Fig. 5) are advantageously used. Calibration is performed in the same way and the use of balanced detectors (see Fig. 6) is also the same as with ac voltage.

However, the observation of the pulses must be performed differently because the 50 (60) Hz time base is missing.

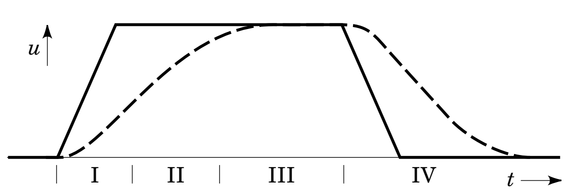

Figure 9. Four stages of switching on and switching off a dc voltage (10). The dotted line represents the growth and decline of internal charge deposits. Only stage III represents a pure dc voltage.

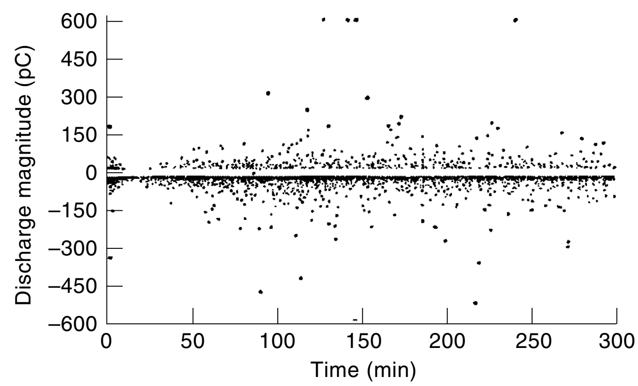

Figure 10. Dc discharges recorded at their appearance (30). Because of their infrequent appearance, these discharges are recorded for a considerable length of time.

Observation of Dc Discharges. There are many ways to display dc discharges, they all have in common that they take far more time than the usual observation of ac discharges. One of the simplest displays shows the magnitude q of the discharges at the time of their appearance (see Fig. 10). This display gives a useful first check, but does not reveal much about the nature of the discharges. It is also utilized during the calibration procedure.

A better observation of dc discharges is made in a diagram where the repetition rate n is recorded as a function of the discharge magnitude q (see Fig. 11). This diagram gives more information, and it also helps to evaluate the danger of the discharges (see the section on evaluating dc discharges). More advanced ways of presentation are also shown in that section.

ELECTRICAL DETECTION IN MORE DETAIL (AC AND DC)

Straight Detection, Quantitative

The height of the impulse V over the detection impedance Z in Fig. 5 which is measured by the discharge detector is given by

$$V = \frac{q}{a + C\left(1 + \dfrac{a}{k}\right)} \tag{1}$$

It follows from this equation that

1. The height of the impulse is proportional to the discharge magnitude q. Direct reading of the discharge magnitude (expressed in picocoulombs) is thus possible, in contrast to nonelectrical methods.
2. For large samples, the signal is inversely proportional to the sample capacitance: $V \approx q/a$. This makes measuring large samples difficult.
3. The use of a couple capacitance k is crucial, no coupling capacitor (or a small one) leads to a large value for a/k in the denominator, and the signal V becomes too small to be measured. The value of k should be of the same order of magnitude as the sample capacitance a.

The amplitude of the signal is independent of the value of Z (or R if a resistor is used as detection impedance). However if

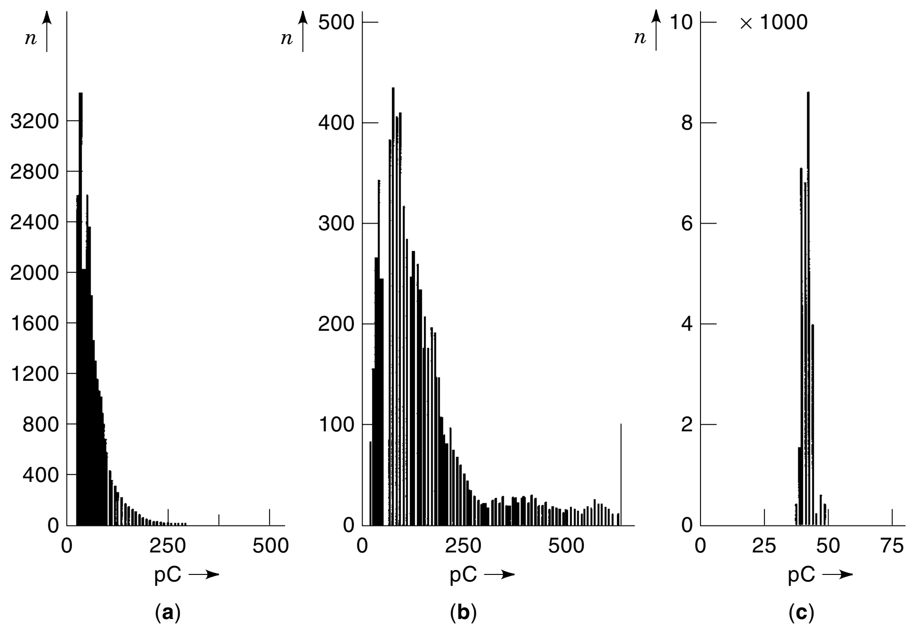

Figure 11. The repetition rate of dc discharges recorded as a function of their magnitude (10). Different types of discharges give different types of diagrams: (a) discharges in a cavity; (b) surface discharges; (c) corona discharges.

Z or R is small, the impulse is too short and the bandwidth of the detector is not sufficient to amplify the impulse. Commercially available discharge detectors, therefore, have variable detection impedances Z that can be matched to the sample capacitance. Usually this matching is realized in five to six steps. Good matching is imperative. For further quantitative relationships, see (1,25,26).

Calibration

Calibrating a detection circuit is relatively simple. A standard charge (e.g., 5 or 50 pC) is injected in the sample and the reading is adjusted to this value. Small standard calibrators are available for this purpose (see, e.g., Fig. 12).

The calibrating pulse must always be injected in the sample, notwithstanding the disadvantages: calibration is done only before or after the test when high voltage is off. Some discharge detectors have a built-in calibrator that injects charges into the detection impedance, so that calibration is performed during the test. This procedure, however, is discouraged because the readings are a factor of $a/(a + k)$ too low, and correcting for this anomaly is usually forgotten.

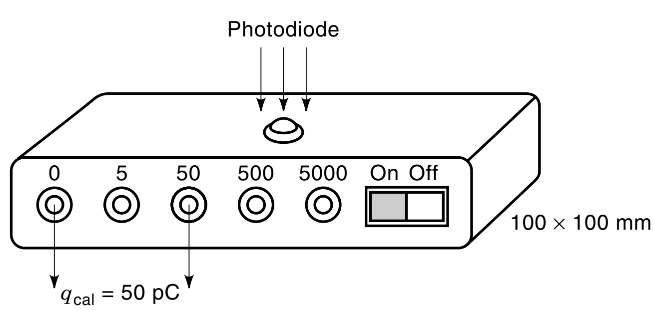

Figure 12. Portable calibrator providing a fixed set of standard charge pulses. The charge pulses are synchronized with the test voltage by a photodiode (1).

Sensitivity

The sensitivity of a detection circuit is defined as the smallest discharge, expressed in picocoulombs, that is just distinguishable from the background noise. To improve the sensitivity, the signal passes a step-up transformer before it is amplified (1). The ratio of this step-up transformer is increased with increasing sample capacitance (see the table following). Most discharge detectors provide this ratio in a number of fixed steps, combined with the choice of the correct detection impedance Z as mentioned previously. These combinations of step-up function and detection impedance are often realized in a set of separate units (to be changed with sample capacitances), called *coupling units* (2) or *quadripoles* (26).

If the correct match is chosen, and if the coupling capacitance k has the same order as the sample capacitance a, the following sensitivities are reached (the sensitivity is then proportional to $\sqrt{a}$):

Sample capacitance	Step-up Ratio	Sensitivity
100 pF	2	0.01 pC
10.0 nF	5	0.1 pC
1.0 μF	45	1 pC

Note that these values are reached only in the absence of any external disturbance and are therefore hard to realize in practice.

Resolution

The resolution of a detection circuit is defined as the smallest time interval between two discharge impulses to be separated by the detector. This resolution is usually in the order of 2 to 10 μs and is checked by observing a corona discharge and increasing the voltage. The distance between pulses [Fig. 7(c)] decreases and the smallest possible distance that can be resolved is determined. The same is done with some calibrators, where the distance between two successive impulses is varied electronically.

Good resolution is essential, because otherwise the discharge patterns of Fig. 7 cannot be evaluated. The resolution should be equal to or better than 10 μs. IEC Standard 270 gives more information.

Balanced Detection, Quantitative

The observations previously made about pulse height, calibration, sensitivity, and resolution also apply to balanced detectors. (1). Balancing is performed by manipulating the R's and C's while a large charge pulse is injected over the bridge. For good balance, the two samples should have the same insulating material, so that their loss factors are equal over a broad frequency spectrum. Capacitances a and a' do not necessarily have to be equal. However, equal capacitances offer optimal results. The conditions for balance are given by

$$\frac{R}{R'} = \frac{a'}{a}$$
$$\frac{C}{C'} = \frac{a}{a'} \tag{2}$$

and

$$\tan\delta = \tan\delta'$$

The quality of balance is defined by the rejection ratio m:

$$m = \frac{\text{response to a charge injected into } a}{\text{response to the same charge injected into } k} \tag{3}$$

The following rejection ratios have been obtained in actual cases:

- Two identical samples: $m = 1000$ to 5000
- Two unequal samples with the same insulating material: $m = 100$ to 500
- Two unequal samples: $m = 3$ to 30

Pulse Discrimination

A variation on the balanced detector is shown in Fig. 13. Pulses that arrive at the same time and with the same polarity are known to originate from outside the sample and are suppressed by electronic pulse discrimination (13). The rejection ratio m is usually less than in a balanced detector, but the circuit has the advantage of simplicity. A balancing procedure is not required. Moreover, instead of using a second sample, disturbing signals are picked up by an antenna and interference from external sources is accordingly suppressed (2,28).

Use of Balanced Detection

An obvious application of these balanced detection methods is measuring discharges in the presence of external disturbances. The true advantage, however, is verifying whether a measured discharge signal arises from within or from outside the sample. This is accomplished by using the switches S and S', by varying the impedances R and R' in Fig. 6, or by disengaging the common mode rejection in Fig. 13. In both cases, external discharges respond heavily to these changes, whereas internal discharges hardly do so. This verification is not achieved by straight detection. It also functions with small rejection ratios, so that an asymmetric bridge (e.g., with $m = 3$ to 30) or common mode rejection (e.g., with $m = 10$) is used.

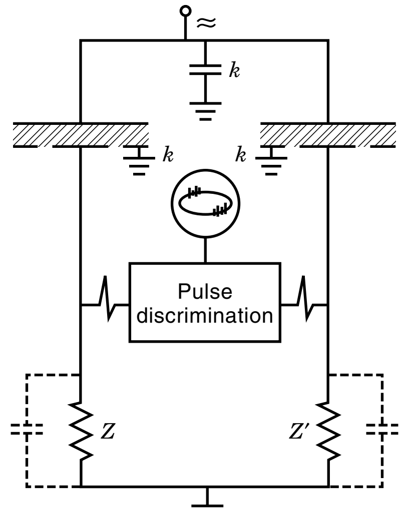

Figure 13. Pulse discrimination: common mode signals are rejected so that discharge signals from outside (from capacitance k or the HV source) are suppressed (9). A digital discriminator transmits or blocks the pulses depending on the timing and the polarity of two incoming pulses.

EVALUATION OF AC DISCHARGES

The Concept of Discharge Magnitude

The charge displacement q is measured in the leads to the sample and *is not equal to the displacement of charge q_1 at the site* of the discharge, as follows from Fig. 14. It is questionable whether this parameter is a good measure for partial discharges. Much has been written on this subject and many proposals have been made, but high-voltage engineers have always returned to q as the preferred definition of discharge magnitude. There are two reasons for this choice: the relationship with energy dissipation in the discharge and the relationship with the physical size of the discharging defect. Both are discussed next.

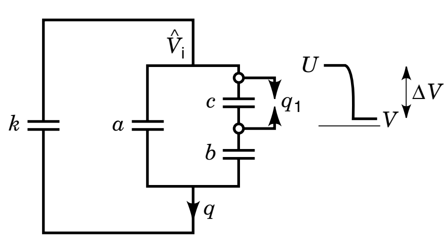

Figure 14. Model circuit for internal discharges. a represents the sample capacitance, c the capacitance of the cavity (or another defect), and b the capacitance of the dielectric in series with the defect (9).

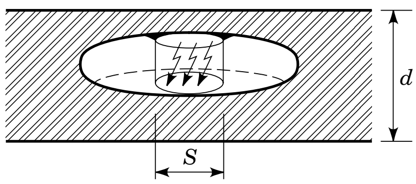

Figure 15. The discharge magnitude q is directly related to the volume occupied by the partial discharge (9).

Energy Dissipation and Physical Size of a Discharge

The energy p dissipated in a discharge and which endangers the insulation is given by (9):

$$p \approx 0.7\, q\, V_i \tag{4}$$

where q is the measured discharge magnitude and V_i is the discharge inception voltage. The deteriorating energy is thus directly proportional to the discharge magnitude q.

The volume of a partial discharge, similarly, is related to the discharge magnitude q by (9)

$$S\Delta V \approx \frac{dq}{\epsilon_0 \epsilon_r} \tag{5}$$

where S is the surface of the discharge site according to Fig. 15, ΔV is the breakdown voltage of the discharge gap and d is the thickness of the dielectric. As ΔV increases with increasing length of the discharge gap, ΔV is proportional to the volume of the discharge. Hence, this volume is proportional to the discharge magnitude q. Examples of the volume of a cavity, as it relates to the expected discharge magnitude, are derived from the previous formula.

Example 1. A discharge magnitude of 1 pC is about the smallest quantity required by industrial tests. This value corresponds to a cavity or surface discharge of about 0.5 × 0.5 × 0.5 mm.

Example 2. A relatively large discharge of 100 pC corresponds to a defect of about 3 × 3 × 1 mm. Both examples are for a dielectric of 10 mm thickness with a dielectric constant of 2.2. These examples show how sensitive discharge detection is in recognizing small defects.

Evaluation of Ac Discharges

After a discharge is measured, the question must be answered whether the discharge is a serious threat to the dielectric. A number of remarks can be made here.

1. To begin with, not too much attention must be given to the precise value of the discharge magnitude. In terms of danger for the dielectric, it is the order of magnitude of the discharge rather than its precise value that controls its effect on the insulation: 1 to 3 pC, 3 to 10 pC, 30 to 100 pC, and so on. Most test specifications for industrial products specify discharge limits on the order of 1 to 10 pC. Evaluation in that case consists of making a voltage diagram, as in Fig. 8 and checking whether the full curve remains below or exceeds the specified limit A.
2. Then the type of discharge has to be determined. For instance, corona discharges may be harmless, whereas discharges in cavities are usually detrimental. Recognizing these discharges is achieved by reading the discharge patterns, as in Fig. 7, but more advanced recognition techniques are available as discussed in a later section.
3. An extremely important variable is the ac *operating stress* in the dielectric. If a higher operating stress is chosen, a lower discharge magnitude must be required. This is illustrated in the following list (9) where permissible discharge magnitudes for extruded dielectrics are given for varying operating stresses.

Operating Stress	Permissible Discharge
< 1.5 kV/mm	no test required
2 kV/mm	100 pC
2.5 kV/mm	30 pC
3 kV/mm	5 pC
3.5 kV/mm	1 pC
> 4 kV/mm	1 pC and overvoltage test

It follows from this list that the requirements rapidly grow more demanding as the operating field strength increases. Over 4 kV/mm, discharge tests are not sufficient, and additional testing is required.

4. The insulation material also is important. Synthetics are sensitive to discharges, whereas glass or porcelain is discharge-proof. Where discharge limits of 1 to 10 pC are specified for components of synthetic material, thousands of picocoulombs are acceptable for glass or porcelain. Machine insulation with a high mica content falls in between (14).
5. Another variable is the frequency of the ac voltage. Radar cables operated at extremely high frequencies do not tolerate discharges at all. On the other hand, fairly large discharge magnitudes may be acceptable at zero frequency, as is seen with dc voltage discharges.

Digital Recognition of Ac Discharges

The recognition of discharges by oscilloscope, as shown in Fig. 7 has its limits. It covers a limited number of discharge types, and it requires an experienced operator. Computer-aided techniques have improved the recognition of discharge patterns by using statistical methods.

Many authors, see for instance (2) and (27), follow a procedure where *statistical distributions* are derived from the discharge patterns. An example is shown in Fig. 17: Here the number of discharges (H_n) and the average magnitude of discharges (H_q) are shown as a function of the time of occurrence (or the phase angle φ). These distributions are often combined in a three-dimensional diagram, as shown for instance in Figs. 24 and 27. Such *distributions* are often far more characteristic for their origin than the conventional discharge *patterns*. In (27) a successful approach has been published.

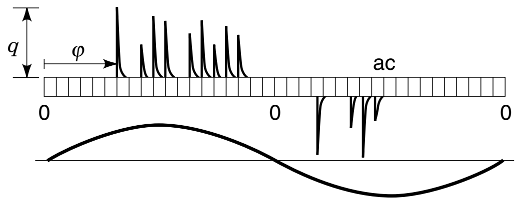

Figure 16. Statistical analysis of ac discharges. In any phase window φ, the number n and the size q of the discharge is stored (10).

A further automized procedure can be found in Refs. 15, 16, and 26). This procedure involves four steps which will be described below:

1. Statistical distributions are made from these patterns.
2. Then the shape of these distributions is characterized by mathematical operators.
3. Combinations of these operators form fingerprints.
4. The fingerprints of unknown and known discharges are mathematically compared with each other.

These four steps are discussed further here.

Statistical Distributions. The complete information about a discharge pattern is incorporated in the *phase angle* φ and the *magnitude q of each pulse* in the pattern (see Fig. 16). (The phase angle φ corresponds to the site on the high-voltage sine wave where the discharge ignites.) This information is converted into statistical distributions. Such distributions may be (see Fig. 17)

1. the pulse count distribution H_n which shows the number of discharges as a function of phase angle φ;
2. the pulse height distribution H_q which shows the average magnitude q of the discharges as a function of the phase angle φ;
3. Other distributions are also used, for instance the maximum pulse height distribution, which shows the maximum discharge measured at a phase angle φ.

Because the distributions in the positive and negative half are considered separate, a great number of distributions is created in this way. The examples given here lead to six different distributions characteristic of a particular discharge.

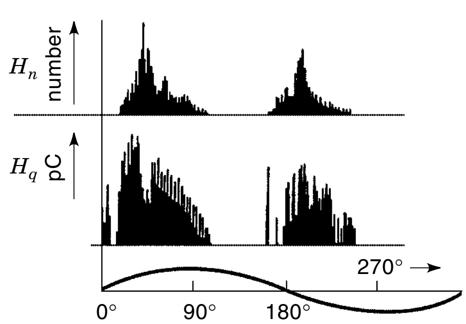

Figure 17. Statistical distributions of ac discharges (9): H_n shows the number (repetition rate) of the discharges in each phase window; H_q shows the average magnitude of the discharges in each phase window.

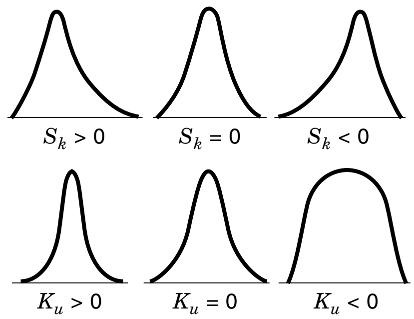

Figure 18. The shape of any of the statistical distributions of Fig. 17 is characterized by operators like skewness S_k and kurtosis K_u. Skewness describes the asymmetry of a distribution and the kurtosis describes the sharpness of a distribution (9).

Recognition Dependent on Operator. Many high voltage (HV) engineers use these distributions and analyze them by eye (2,27), similarly to recognizing discharge patterns on an ellipse, as in Fig. 7. The distributions are often displayed in a three-dimensional diagram as in Fig. 24 and 27, and they have quite characteristic features. Although better than examining the ellipse, this procedure is still too dependent on personal interpretation. Therefore, further automation has been worked out as described here.

Statistical Operators. Each distribution is further analyzed by a number of *statistical operators.* The following operators are used:

1. *Skewness.* The skewness S_k represents the asymmetry of the distribution. If the distribution is symmetric, S_k is zero. If it is asymmetric to the left, as in Fig. 18, S_k is positive and if it is asymmetric to the right, S_k is negative. The more asymmetric the distribution, the higher S_k.
2. *Kurtosis.* The kurtosis K_u represents the sharpness of the distribution (see Fig. 18). If the distribution has the same shape as a normal distribution, the kurtosis is zero. If it is sharper than that, K_u is positive, and, if it is flatter, K_u is negative.
3. *Number of peaks.* The number of local peaks P_e in the distribution may also be chosen as an operator. In the examples of Fig. 17, this number may be, respectively, 1, 1, 3, and 4.
4. *Cross-correlation.* The *cross-correlation factor* expresses the difference in shape between the distributions in the positive and the negative halves of the sine way.

Fingerprints. The previous statistical operators are applied to the various distributions. Many combinations of operators and distributions can be made, such as the skewness of H_n^+, H_q^+ and other distributions; the kurtosis of H_n^+, H_q^+ and other distributions; the number of peaks in H_n^+, H_q^+, and the cross-correlation between H^+ and H^-. A great number of operators are calculated in this way, and together they form the fingerprint of that discharge. In actual cases, up to 30 operators have been used. The fingerprint of a discharge thus consists of a series of (up to 30) positive or negative numbers which describes the *general shape* of the discharge pattern.

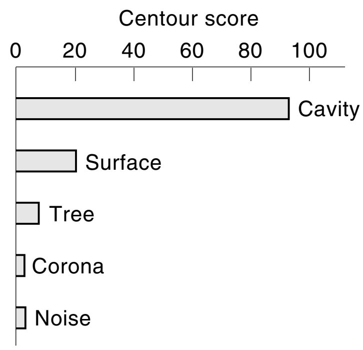

Figure 19. Classification of an ac discharge by centour score (10). An unknown discharge pattern is recognized here as originating from discharges in a cavity.

Recognition. In a last step, the fingerprint of an unknown discharge is compared to a database of fingerprints of discharges of known origin. Examples of known discharges, for instance, are artificial cavities in a dielectric model or natural discharges in a full-size component.

A good algorithm for comparing the fingerprints is the centour score (16,33). Here a fingerprint is represented by a data point in a 30-dimensional space. In the database, a characteristic defect is characterized by a cloud of dots, measured for several samples of that particular defect. The unknown defect is characterized by only one data point. The centour score is defined as the percentage of data points farther away from the cloud's center of gravity than the single data point of the unknown discharge.

The centour score is expressed as a percentage varying from 0 to 100%. It *is not* equal to the probability that two discharges are identical, but it reflects their similarity. An example of recognition by centour score (10) is given in Fig. 19, where a discharge in a dc component is recognized as caused by a cavity in the insulation.

EVALUATION OF DC DISCHARGES

Evaluation

There are hardly any official specifications for testing dc equipment. A requirement exists for power transformers in ac/dc converters, which sets a limit for a *maximum discharge magnitude,* for example, 1000 pC at a specified repetition rate, for example, less than 1 discharge per minute (see also a section on dc in ASTM D1868-93).

A recently proposed acceptance test for dc components records the repetition rate n of all discharges larger than a threshold value q_{th} as shown in Fig. 20. In this diagram, a line is drawn where acceptable limits for the repetition rate and the discharge magnitude are specified. Results over this line are regarded as unsafe, and results below this line are acceptable (10). A tentative value of 2 $nC \cdot min^{-1}$ is chosen, but the line can be adjusted to higher or lower values for specific objects. The diagram of Fig. 20 plays the same role for dc as the discharge-voltage diagram of Fig. 8 for ac. For some specific products, this borderline has been given a specific value (see the sections on dc power cables and nonenergy components).

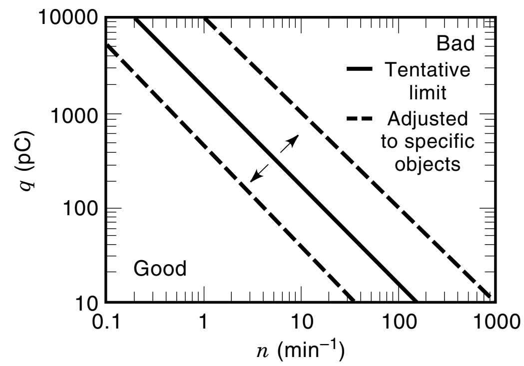

Figure 20. Recording dc discharges: the magnitude of the discharges q is recorded as a function of their repetition rate n. The diagram is on a logarithmic scale. A straight line **K** then is drawn to distinguish between "good" and "bad" objects. Recordings above line **K** represent objects which are not acceptable. Line **K** itself is shifted according to the experiences with specific types of objects (12).

Computer-Aided Recognition of Dc Discharges

In contrast to ac discharges, evidently no information on a phase angle φ exists. It has been recognized (11) that for dc the role of φ can be assumed by the time interval Δt between discharges (see Fig. 21).

One further step forward is to distinguish between a time interval to the next discharge, called Δt_s (s = successive), and a time interval before the last one, Δt_p (p = preceding). These successive and preceding time intervals take the place of the phase angles φ in the positive and negative half-cycles of an ac voltage. Then all classification and recognition techniques developed for ac voltage can also be used for dc discharges (11,26). See the sections on dc capacitors and dc nonenergy components.

DISCHARGE TESTS ON ACTUAL AC EQUIPMENT

Power Transformers

The combination of the self-inductances in the windings and their capacitances to earth gives a traveling-wave character to the windings (1,24). When a partial discharge takes place, traveling waves wander through the windings. These waves contain frequencies lower than a cutoff frequency ω_c. The attenuation of the discharge signal above ω_c is large, whereas low or no attenuation takes place at frequencies below this limit. In actual cases, ω_c amounts to about 200 kHz. It is therefore beneficial to use a discharge detector with an input frequency below 200 kHz. Several commercially available detectors have a choice in input frequency so that this requirement is satisfied. Low attenuation factors, better than two to one, are obtained this way.

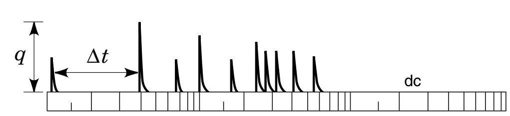

Figure 21. Statistical analysis of dc discharges (10). The size q and the number n of the discharges are recorded as a function of the time lag Δt. The time lag is recorded on a logarithmic scale. Note the similarity to Fig. 16 on ac discharges.

When testing a power transformer, the test voltage is applied in two different ways, as shown in Fig. 22: (1) in the induced-voltage test, the transformer is energized by feeding the low-voltage windings. The test voltage may be twice the nominal voltage. Then the frequency of this voltage is doubled to prevent saturation of the magnetic core. This has no effect on the detection circuit because the discharge signals remain the same, but the time base of the detector should also be adjusted; (2) in the *applied-voltage test,* the test voltage is applied to the high-voltage bushing. In both cases coupling to the detector is performed by an impedance at (a) in the ground lead, or by a coupling capacitor and an impedance at (b) (see Fig. 22). In the latter case, a bushing tap is often used. Because several bushings and ground leads are available, several calibrations are made. Either the lowest or an average response is taken as the representative calibration. CIGRE recommendations for these calibrations are found in Ref. 19. Detection sensitivity of 50 pC is recommended.

Pattern recognition by digital analysis is performed well for power transformers. During testing, the discharge patterns before, during, and after the induced voltage test are compared. If the patterns remain the same at these stages, the insulation is considered safe. However, this judgment is subjective and depends too much on the operator's personal opinion. A better comparison is made with the $H_n(\varphi, q)$ distributions (8), as discussed previously.

However, a still better practice is to use automatic recognition by feature extraction (see the preceding section). In (8) a number of transformers in good condition are compared with each other, and the patterns are recognized to be of the same origin. This is shown in Fig. 23, where all sound transformers score better than 75%. Insulation in good condition is defined this way. Two 55 MVA reactors and a 203 MVA transformer in this picture do not show any recognition. The 55 MVA reactors proved to have a damaged screen. The 203 MVA transformer was further tested for irregularities. In this way a manufacturer assembles a data bank on sound and faulty transformer insulation and stores its experience.

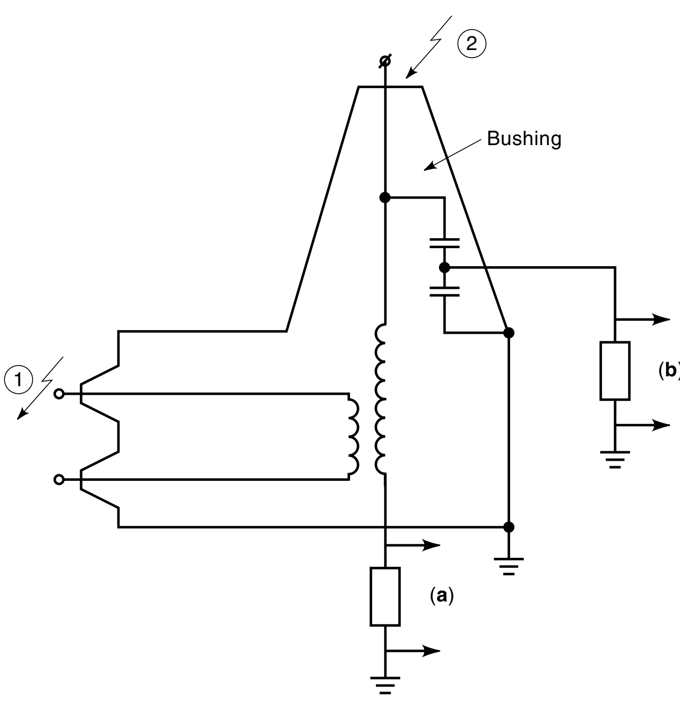

Figure 22. Discharge detection on a power transformer (1). The ac discharge signals are either taken from a ground lead (a) or from a bushing tap (b). At position 1 the induced voltage test is shown and at position 2 the applied voltage test.

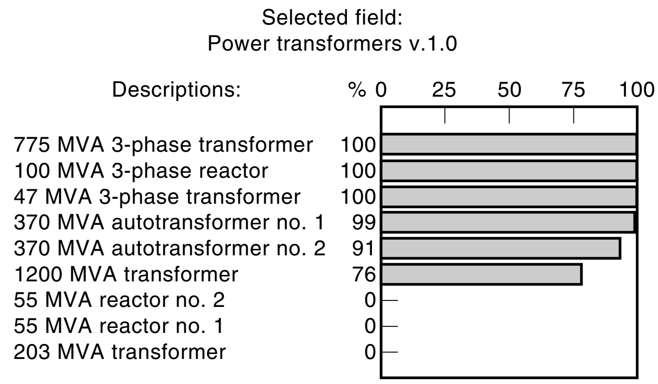

Figure 23. Recognition of ac discharges in power transformers by centour score. The similarity of the discharges in the first six transformers is clear. These discharges represent transformers in good condition. The discharges in the other three objects are of a totally other nature and these objects are further tested for their quality (30).

Rotating Machines

Three situations can be distinguished: (1) Discharge testing of separate bars which takes place during manufacturing. Measurement of tan δ plays an important role here (25). (2) Testing of complete machine insulation. This takes place after assembling a machine and is also performed at regular intervals during service. (3) Testing with probes built into the stator slots (30).

1. The stator coils form a network similar to that of transformers (24, Chap. 8). Discharge impulses generated in the insulation are attenuated traveling to the terminals. Again, low-frequency detection is recommended. With a frequency band up to 100 kHz, low attenuation factors of 2 to 3 are quoted (1). Binder (14) has given simple guidance on the acceptability of these discharges during service:
   1. Discharges up to 1000 pC are acceptable.
   2. Discharges of 10 nC shall be located and the appropriate machine bar shall be replaced when convenient.
   3. Discharges of 100 nC are unacceptable and the machine shall be stopped to replace the faulty insulation.
2. Pattern recognition is also useful for complete machine insulation. Comparison of the three-dimensional pictures of the $H_n(\varphi, q)$ distributions (see Fig. 24) gives useful information about the phase where irregularities occur. The same result follows from automatic recognition using the fingerprint technique (22). Care must be taken in dealing with crosstalk between the windings.

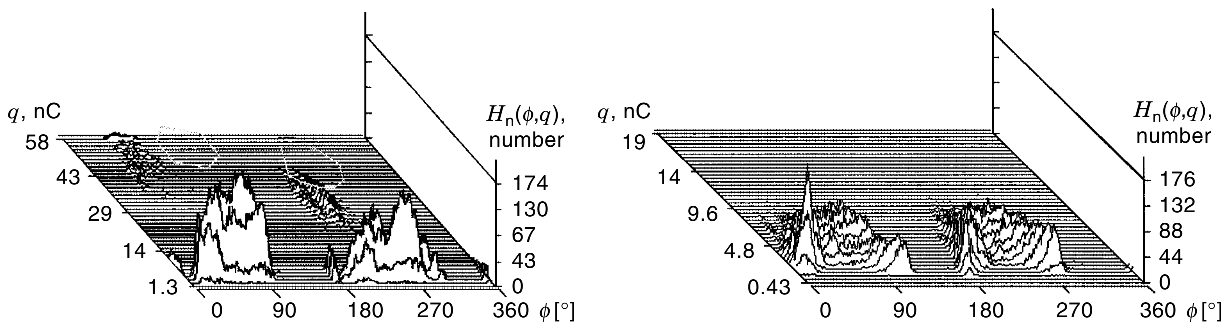

Figure 24. Three-dimensional distributions of ac discharges in the stator insulation of a large turbogenerator (30). Left: phases U and W; right: phase V. Optical comparison shows a great difference between the two sound phases and the faulty phase V.

3. Sometimes probes are built into the slots of the stator. Stone (30) gives a survey of detection methods and describes a 1 MHz slot coupler which is instilled *under the wedge* of the top bar or *between top and bottom bars*. The discharges are observed with a very wide band detector. Noise elimination is based on the differences in pulse shape: Internal discharges have a width of less than 6 ns, whereas noise impulses have a width larger than 8 ns. This way of measuring eliminates noise and can directly distinguish between discharges in the slot and those in the end-turns and also differentiate between different types of discharges.

Gas-Insulated Switchgear

Gas insulated switchgear (GIS) up to 170 kV rated voltage is often built in three-phase construction, which preferably is tested with three-phase voltage. Only then is the field configuration identical to that in actual service. If no three-phase voltage is available (one of the reasons may be the high cost of test equipment), single-phase testing is performed.

Three-Phase Testing. The three phases are connected to the detector by coupling capacitors (see Fig. 25), and a balanced detector is used (1). (Bushing taps are used for coupling if bushings are available). In the circuit shown here, discharges between phase R and ground are rejected, and those between S and T are doubled. By rotating the three connections, discharges are located in one of the three phases. More combinations are made offering more possibilities for discharge location (21).

Single-Phase Testing. One phase is stressed at nominal voltage (or some 30% higher for safety reasons), and discharges between the poles are measured. The insulation to ground is overstressed in this situation and therefore the discharges to ground are rejected by a balanced detector (see Fig. 26) (20). After that, the test voltage is lowered to phase voltage $U/\sqrt{3}$ and the detector is switched over to straight detection. Now the discharges between pole and ground are measured at their proper voltage. The connections are rotated to test the three poles. Another possibility, with a better field configuration, is described in (1).

Single-Phase Constructions. GIS for rated voltages from about 170 kV upward is usually built as single-phase construction. Then the detection circuit is straight, as shown in Fig. 5. Good results are also obtained with ultra-wide band detection. This is increasingly used for on-site tests; see for instance (31) and (32).

For all of these tests high sensitivity is recommended. No discharges larger than 1 to 3 pC are acceptable. Automatic pattern recognition in GIS gives adequate results. Most experience has been obtained with artificial defects, because natu-

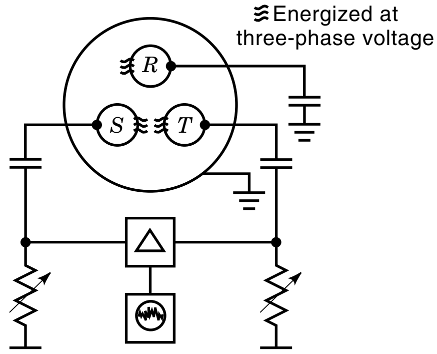

Figure 25. Three phase testing for ac discharges in a three-phase GIS construction (1).

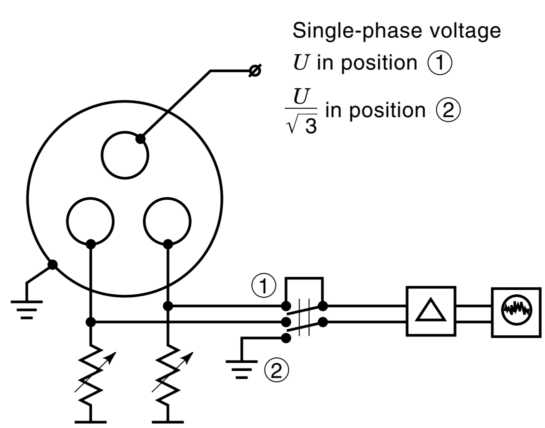

Figure 26. Single-phase testing for ac discharges in a three-phase GIS. Position 1 balanced detection and position 2 straight detection (1).

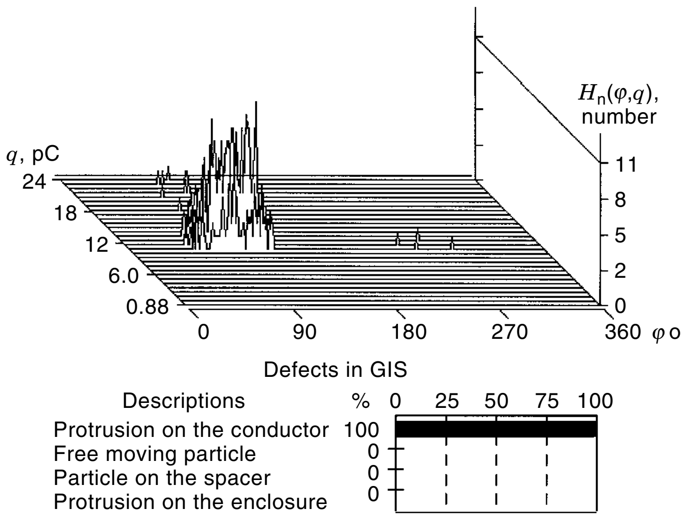

Figure 27. A three-dimensional diagram and the results of the centour score of ac discharges in GIS (30). The nature of the defect is clearly indicated by the centour score.

ral defects in GIS are quite rare. Recognition of a protrusion at the conductor is shown in Fig. 27 (23).

Ac Power Cables

With conventional detection, a cable is measured as if it were a lumped capacitor. If the cable, however, is longer than one to two hundred meters, traveling waves play a role. A discharge causes pulses to travel in two directions, and these pulses are reflected at the ends and arrive one after the other at the detector (see Fig. 28). Superposition of these pulses causes appreciable errors when measured with a conventional detector. CIGRE (21) gives recommendations for reducing these errors, and modern detectors (2) comply with these recommendations.

The traveling waves are also used to *locate* the defect. A moderately wide band, for example, 5 MHz, is used to separate these pulses and to measure the time interval T between pulses. The location of the defect is found by

$$2x = vT \tag{6}$$

where x is the distance of the defect to the far end of the cable and v is the wave velocity (1). Many discharge detectors (2) have this facility nowadays. Moreover, shorter cables, down to 20 m, have been measured in this way as well, but with band widths up to 500 MHz.

Routine tests on cables are usually made with straight detection circuits. Type tests are performed in balanced detection. By making interruptions in the sheath, separate measurements are made of the cable, the terminals, and of other accessories (9) (see Fig. 29). Because discharge detection is mainly a check for *synthetic insulated* cables, high sensitivity is chosen, on the order of one to several picocoulombs, and no discharges higher than this sensitivity level are acceptable.

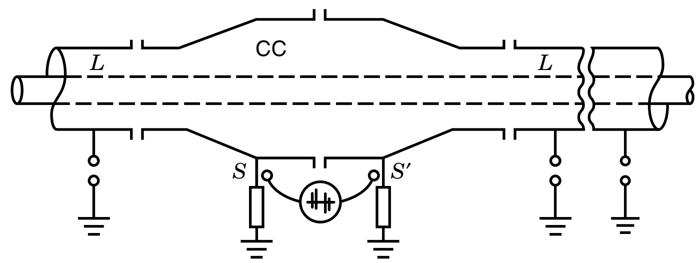

Figure 29. Location of ac or dc discharges by subdivision of the electrodes (9). The cable connector **CC** is divided in two halves and is separated from the cable length **L**. Manipulating the balance in the balanced detector (see Fig. 6) may reveal the site of the discharge: at the right or the left-hand side of the connector or of the cable length. Further subdivision is accomplished to pinpoint the discharge.

Pattern recognition by digital analysis works well with extruded power cables. Fig. 30 shows an example of a discharge in a 70 kV crosslinked polyethylene (XLPE) cable. The distributions were observed in a two-minute test at nominal voltage. The results of the centour score analysis show clearly that the discharge was caused by a cavity at the ground screen (30).

Ac Power Capacitors

Power capacitors can adequately be tested with conventional discharge detectors. However, the coupling capacitor usually provided with these detectors (1 to 10 nF) is too small for adequate sensitivity. The coupling capacitor k shown in Fig. 5 should be of the same order of magnitude as the sample. Usually a second capacitor of the same batch is used for this (and consequently is also measured also). If, however, two equal capacitors are measured at a time they can also be introduced in a balanced circuit (see Fig. 6), so that disturbances are rejected and the sensitivity is improved.

Discharges in paper-insulated capacitors are caused by imperfect drying or impregnation. Moreover, overstress from atmospheric or switching surges causes surface discharges at the edges of foils. Both types of defects are uncovered if the capacitor is tested at 1.5 times nominal voltage at a sensitivity of 50 pC. Plastic-insulated capacitors are tested at lower sensitivity levels of 5 to 10 pC (1).

DISCHARGE TESTS OF ACTUAL DC EQUIPMENT

Dc Power Cables

High-voltage dc cables, also called HVDC cables, are usually paper-insulated. Discharge tests on these cables are rare.

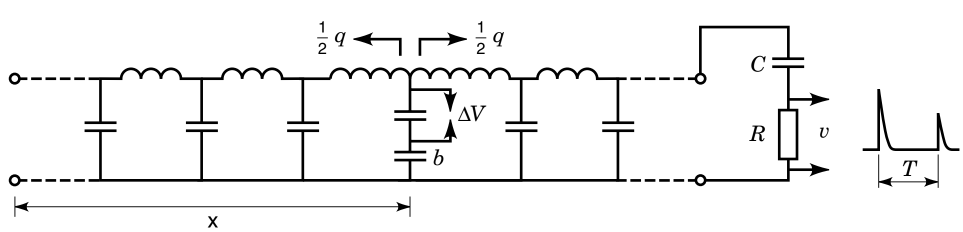

Figure 28. Location of discharges by traveling waves. The time lag T between a direct wave and its reflection is measured. The distance x of the defect to the far end of the cable is $2x = Tv$, where v is the wave velocity (9).

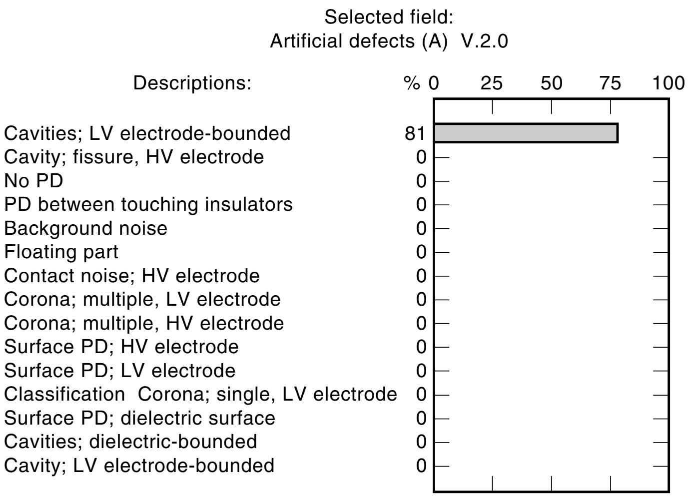

Figure 30. Recognition of ac discharges in a 900 m long XLPE cable (29). The centour score points clearly to multiple cavities which are adjacent to the grounded electrode.

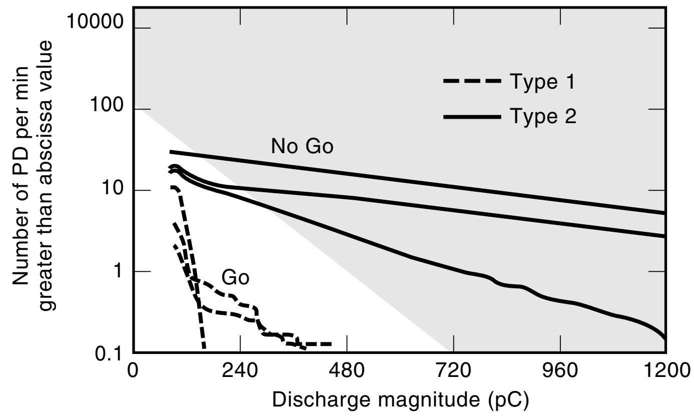

Figure 32. Evaluation of dc discharges in x-ray transformers in a q–n diagram as in Fig. 31. A distinction is made between samples that had to be rejected and samples that might pass the test (11). (Note that the scale for the discharge magnitude is nonlogarithmic, which makes drawing a borderline between Go and No Go more difficult.)

Ekenstierna (28) has shown that breakdown in overvoltage tests is predicted by dc discharge detection. Discharges over 1 nC with a repetition rate of more than 1 min^{-1} are detrimental and initiate breakdown. Jeroense (12) has shown that a distinction can be made between properly used and overloaded cable. The q–n diagram of properly used cables lie below the line 0.5 $nC \cdot min^{-1}$, and overloaded cables lie over that line, as shown in Fig. 31. This criterion may also be used to discriminate between well-manufactured and less satisfactory cables.

Dc Nonenergy Equipment

High-voltage dc is often applied in nonenergy equipment, like x-ray tubes and generators, television tubes and sets, electron microscopes, and many other devices. There is an increasing interest in using discharge detection for these components as voltages go up and sizes go down. Nonenergy dc equipment is readily tested with the circuits and the techniques laid down in the first sections of this article. Distinction is made between sound and faulty components and, if discharges are present, the type of defect is determined. In (11) an example is shown of the distinction between good and faulty insulation of x-ray filament transformers (see Fig. 32). An acceptance limit of about 600 $pC \cdot min^{-1}$ is derived from this picture.

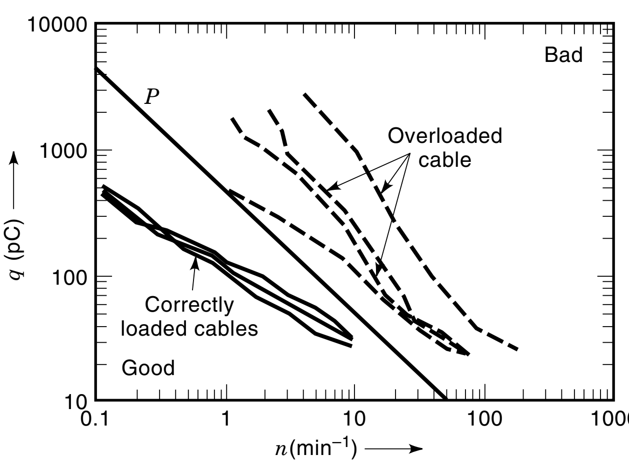

Figure 31. Evaluation of dc discharges in a q–n diagram according to Fig. 20. High-voltage dc cables were measured and were classified as cables of "good" or "bad" quality (12).

FURTHER DEVELOPMENTS

Monitoring

The techniques previously studied are used mainly indoors in high-voltage laboratories for development and testing. This field is well developed and has crystallized in a number of specifications (IEC, CIGRE, ASTM, etc.) for measuring techniques and their application to specific components, such as high-voltage cables, power transformers, heavy switchgear. Commercial discharge detectors for this purpose are widely available.

Another category of measurements is still in development, the monitoring and assessment of high-voltage components in the field. These measurements suffer from the harsh electrical environment in power stations and substations. There is still much development going on, but few methods have attained general acceptance. The main topics of research are coupling, filtering, pattern assessment and ultra-wide band detection.

Research

Discharge detection for research purposes aims at extremely wideband observations, combined with optical detection. The wideband circuits in principle are equal to the basic circuit of Fig. 5, but much care must be taken to prevent loops, unwanted self-inductances, cross talk, and so on. The optical techniques have been developed to observe discharge tracks, in time (down to nanoseconds and less) and in space (down to microscopic dimensions). These observations may be completed with chemical analyses. The main characteristics of partial discharges are revealed by these techniques in this way, for both ac voltage (6) and for dc voltage (11).

BIBLIOGRAPHY

1. F. H. Kreuger, *Partial Discharge Detection in High-Voltage Equipment.* Butterworth, London 1989; first version 1964.
2. Information bulletins of ADWEL, Biddle, Haefely, Hippotronics, IRIS, LDCI, Mitshubishi, *PD*, Robinson, SEFEMI, Tettex and many others.
3. H. Kawada et al., Partial discharge monitor for oilfilled transformers, *Proc. IEEE* **PAS 103** (2).
4. Y. Takahashi, Diagnostic methods for gas insulated substations. *IEEE Trans. Electr. Insul.* **EI-21** (6): 1986.
5. F. H. Kreuger and P. H. F. Morshuis, Optical detection of surface discharges, *IEEE Trans. Electr. Insul.* **23** (3): 1988.
6. P. H. F. Morshuis, *Partial Discharge Mechanisms,* Thesis, Delft: Delft University Press, 1993.
7. CIGRE, Recognition of discharges. *Electra* No. 11, 1969.
8. E. Gulski et al., Digital tools for PD analysis during induced tests of large power transformers, *IEEE Annu. Rep. Electr. Insul. and Dielectr. Phen.* Oct 1996.
9. F. H. Kreuger, *Industrial High Voltage,* Delft: Delft University Press, 1991/92.
10. F. H. Kreuger, *Industrial High DC Voltage,* Delft: Delft University Press, 1995.
11. U. Fromm, *Partial Discharge and Breakdown Testing at High DC Voltage,* Thesis, Delft University Press, Delft, 1995.
12. M. Jeroense, *Partial Discharges and Charges in High Voltage DC Cable,* Thesis, Delft University Press, Delft, 1997.
13. D. A. Hilder, Partial discharge measurements in harsh electrical environments, *CIGRE symposium* May 1987, paper 700-06.
14. E. Binder, Techniques for discharge measurements in stator windings of generators, *CIGRE symposium* May 1985, paper 700-03.
15. E. Gulski, Computer Aided Recognition of Partial Discharges Using Statistical Tools, Thesis, Delft University Press, Delft, 1991.
16. A. Krivda, Recognition of Discharges, Thesis, Delft University Press, Delft, 1995.
17. *IEC Publication* 270, Standard on partial discharge detection.
18. CIGRE, Calibration procedures for analog and digital partial discharge measuring instruments, *Record of CIGRE WG 33.3 Conference "H.V. Test and Measuring Techniques"* Winchester, UK, Sept. 1996.
19. CIGRE, Recommendations for partial discharge measurements on transformers and reactors, *Electra* 19 and 21, 1971.
20. F. H. Kreuger, Three phase discharge detection, *CIGRE Symposium* May 1987, report 700-05.
21. CIGRE, Discharge measurement in long length of cable, prevention of errors, *CIGRE* 1968 Paper 21-01, p. 23.
22. E. Gulski and A. Zielonka, Application of digital partial discharge measuring techniques for the diagnoses of high voltage generator insulation, *Conf. Rec. of the 1996 IEEE Int. Symp. on Electr. Insul.* Montreal/Quebec, June 1996.
23. F. H. Kreuger, E. Gulski, and W. A. Sonneveld, Diagnosis in GIS by statistical analysis of discharges, *CIGRE,* Paris, paper 15/23-04, 1992.
24. D. König and Y. Narayana Rao, *Partial Discharges in Electric Power Apparatus.* VDE Verlag, 1993.
25. R. Bartnikas and E. J. McMahon, *Engineering Dielectrics* 2nd. ed. Philadelphia: ASTM 1979, 1984 Vol. I.
26. Haefely-Tettex: *TEAS discharge analyzer* .
27. B. A. Fruth and D. W. Gross, Partial discharge signal generation transmission and acquisition, *IEE Proc. Science, Meas. and Techn.,* **142** (1): 1995.
28. A. Erikson and B. Ekenstierna and others, Development concerning testing procedures of mass-impregnated HVDC cable, *CIGRE* 1994, rep. 21-206.
29. Internal reports, High Voltage Laboratory, Delft University of Technology, Delft.
30. G. C. Stone, Tutorial on rotating machine discharge testing, *Cigré/EPRI Colloquium on Maintenance and Refurbishment of Utility Turbogenerators, Hydrogenerators and Large Motors,* Florence, Italy, April 1997.
31. B. F. Hampton and R. J. Meats, Diagnostic measurements at UHF in gas insulated substations, *IEEE Proceedings,* **135**, Pt. C, No. 2, 1988.
32. J. S. Pearson et al., Partial discharge diagnostics for gas insulated substations, *IEEE Trans. Diel. and Electr. Insul.* **2** (5): 1995.
33. A. Krivda, Automated recognition of partial discharges, *IEEE Trans. Diel. and Electr. Insul.* **2** (5): 1995.

F. H. KREUGER
P. H. F. MORSHUIS
Delft University of Technology